Effect of Latent Heat Release and Capillary Anisotropy in Dendrite Formation of Al-Cu Alloy Crystallization

Mary Grace Kalnay[a], **Isaac Fiore**[a], **and Dr. Nikolas Provatas**[a]

[a]Department of Physics, McGill University, 3600 Rue Université, Montréeal, QC, H3A 2T8, Canada

This manuscript was compiled on April 9, 2017

This project aims to study the effects of latent heat release during alloy solidification. An established repository of code which implements phase field modeling to simulate rapid cooling of metal alloy droplets is used to create several simulation cases. The outputs of these computations are then analyzed using Paraview to examine the primary growth directions and morphology of each simulation. Analysis of these simulated crystals show that latent heat release during solidification as well as growth anisotropies help yield distinct types of crystal morphology. Results are relevant as understanding the coupling between temperature with growth kinetics and dendritic morphology is useful in industrial processes.

Dendrites | Crystallization | Latent Heat Release | Alloys | Anisotropy

The use of metal alloy powders and the process of their rapid solidification is being explored with increasing interest. As industries such as aerospace and materials engineering find more applications for these powders, there is high demand for information on the formation and morphologies of their microstructures. The variety of orientations, structures, and chemical compositions on the microscale of the powder heavily influences the mechanical and physical macroscale properties of the solidified metal including toughness, elasticity, corrosion resistance, and electrical conductivity /citecracking . Thus a higher understanding of the formations of these microstructures will yield increased control over the production process of the alloy.

Solidification is an intrinsically out of equilibrium phenomenon (5) which makes it fascinating to observe and characterize. During a solidifying phase transformation, the two phases, solid and liquid, are separated by an interfacial region of width, W typically on the nanometer scale. Atoms from the liquid state are incorporated into the solid state across the interface over a time scale τ. As the liquid is cooled below its melting temperature the liquidous atoms enter a metastable phase before eventually settling and solidifying in place. In this work we a simple two-component system (alloy) that is a mixture of Aluminum (Al) and Copper (Cu). The phase diagram shows in Figure 1, for metal alloys of a given concentration, there exists a region for which both the solid (α) and liquid (L) states can coexist ($\alpha + L$) which is bounded above and below by the coexistence lines.

Starting from the melting point of the correct concentration, the liquid can be undercooled to induce solidification. The process of undercooling takes the liquid metal alloy below the freezing point without a crystal nucleus forming. Crystallization begins with a spherical nucleation site that grows into the undercooled melt. As it solidifies, the morphological instability at the solid-liquid interface produces dendrites, which are highly organized, branched, tree-like patterns (Figure 2). These dendrites have preferential growth directions governed by the surface energy of the solid–liquid interface, -characterized by the capillary length d_0 - as well as the mobility μ of attachment of atoms to the interface on different crystallographic

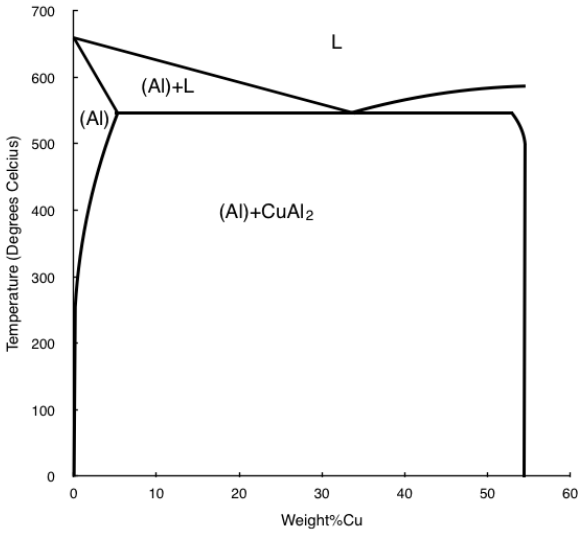

Fig. 1. Phase Diagram of Aluminum-Copper Alloy, where L represents the liquidous phase, (Al) is solid aluminum, and (Al)+L is the coexistence. Created using PAGES software.

planes, or both. The former will be referred to as the kinetic anisotropy, and the latter as the capillary anisotropy. As they solidify, the atoms lose their thermal energy in the form of latent heat released into the undercooled melt. The resulting growth rate and crystal morphology thus depends on the conduction of the latent heat away from the

Significance Statement

With the increased prevalence of processes like 3D printing in large-scale industrial applications, the factors that influence the rapid solidification of metal alloys require more attention than ever before. The crystalline microstructures determine many characteristics of the metal, and set the scale for defects in the durability and ductility of the final product. Accurate simulations of this process provide ample insight as to how industries can alter their solidification processes and produce more quality materials. Here, we demonstrate the influence of capillary anisotropy and latent heat release occurring along the solid-liquid interface to determine the resulting morphological impacts.

[1]Mary Grace Kalnay and Isaac Fiore contributed equally to this work.

[2]To whom correspondence should be addressed. E-mail: isaac.fiore@mail.mcgill.ca, marygrace.kalnay@mail.mcgill.ca

interface.

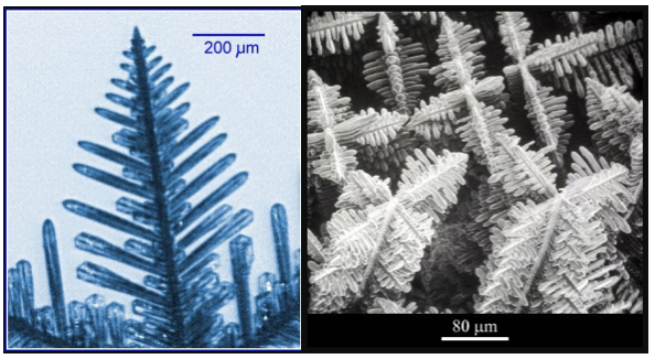

Fig. 2. Example dendrite structures of varying size and composition. On the left, an enlarged image of a snowflake shows the dendrites formed as water freezes under atomic pressure (7). On the right, is an image of the 3D structure of dendrites in a cobalt-samarium-copper alloy as seen by a scanning electron microscope (8).

To characterize the formation of these microstructure dendrites for simulation, the phase-field method is implemented. The phase field model comprises a set of time-dependent differential equations that evolve the dynamics of an order parameter ϕ, which varies between two one constant (-1) in the liquid to (+1) in the solid. The order parameter characterizes the change of phase from disorder (liquid) to ordered (solid). Its evolution is coupled to a diffusion equation that controls the transport of heat and/or solute during solidification. Here we will be examining a two component mixture called an alloy in which it is assumed that temperature is instantaneously updated on the time scale of solute diffusion and change of order. The details of these equations and the numerical algorithm used to solve them is beyond the scope of this project and are discussed in (6). This is an assumption made often in the literature.

The phase-field method also incorporates the effect of capillarity through the interface width W coupled to order parameter gradients and interface mobility through a kinetic time scale τ that controls time derivatives in the order parameter equations.

The anisotropies of W and τ are represented by the equations:

$$\frac{W(n)}{W_o} = 1 + \epsilon_\gamma cos4\theta \quad [1]$$

$$\frac{\tau(n)}{\tau_o} = (1 + \epsilon_\gamma cos4\theta)^2 \quad [2]$$

Where ϵ_γ is the anisotropy strength, and θ is the angle of the local normal to the interface and a reference axis.

The effect of the time scale τ in the phase field equations is to control the effective atomic mobility of atoms across the solid-liquid interface. This is is expressed as a "kinetic coefficient":

$$\beta(n) = \frac{1}{\mu} = \beta o(1 + \epsilon_k cos4\theta) \quad [3]$$

Where ϵ_k is the kinetic anisotropy strength.

These equations both contain a constant term, as well as a cosine term that dictates the directionality of the anisotropy. When anisotropy strength approaches 0, the cosine term approaches 0, but there is still a force that drives crystal growth. This growth however has no coupling with orientation, and as a result the crystal formation lacks dendrites.

The temperature at the interface is represented by:

$$T_i = T_E - d_o(\kappa - \beta)v \quad [4]$$

Where κ is the local interface curvature, capillary length is d_o, and growth velocity is v.

A large body of work has been published to predict the operating state and morphologies of dendritic crystals. Most models, and experiments, have focused on the regime where the solid-liquid interface can be considered in near equilibrium. This is sufficiently slow that one can ignore the role of latent heat in the crystallization and morpho-genisis problem of crystals. This is a particularly bad assumption in the paradigm of rapid solidification.

1. Results and Discussion

To test the effect of latent heat and capillary anisotropy on the solidification process, simulations were run with an existing repository of code provided by Professor Nikolas Provatas and his PhD student Tatu Pinomaa. This code emulates the conditions of Eqs. 1-4 to describe the solidification interface.

Examining the influence of capillary anisotropy and global heat balance produced several simulation cases.

Case 1: Latent Heat.

Latent heat release through global heat balance was conducted with simulations of the previously discussed PDEs where the global heat balance was toggled on and off.

The experimental results, as seen in Figures 3 and 4, demonstrate clear morphological and solidification rate differences. In the presence of a global heat balance, the branches have a stunted growth rate and triangular morphology along the primary axes. When global heat balance is turned off, the solidification is very rapid and while growth along the primary axes is still dendritic, there is visible growth in other directions with similar growth rates producing a rounder less branched morphology. These results support basic theoretical explanations. When global heat balance is included, the energy from the newly solidified molecules is given off as latent heat into the undercooled melt. This increases the temperature outside of the interface, and eventually dissipates throughout the droplet. This added energy creates a higher temperature gradient, prolonging the solidification of the entire system. This systematic behavior reflects the fluctuating temperature at the interface (Equation 4) through peaks and plateaus of the dendrites creating wide triangular patterns, as seen in the bottom left time step of Figure 3. Similarly, when global heat balance is turned off it is expected that the growth rate in all directions should increase. As shown in Figure 5, the simulations without global heat balance have continual heat loss from the system, pushing the solidification to move fast, and producing the large crystals shown in Figure 4. In addition to the large and less refined branches, Figure also shows the presence of a second nucleation site which appears around 3000 microseconds into the simulation. This only further supports the rapid nature of the simulations without latent heat release, as the temperature by 3000 microseconds is low enough to nucleate on its own. When considering the size of the solid structure at equivalent times during the simulation it is apparent that Figure 3 shows stunted growth, compared to Figure 4.

Case 2: Capillary Anisotropy.

The Capillary Anisotropy E_γ from equations 1 and 2, was toggled on and off to determine its affect on the solid morphologies.

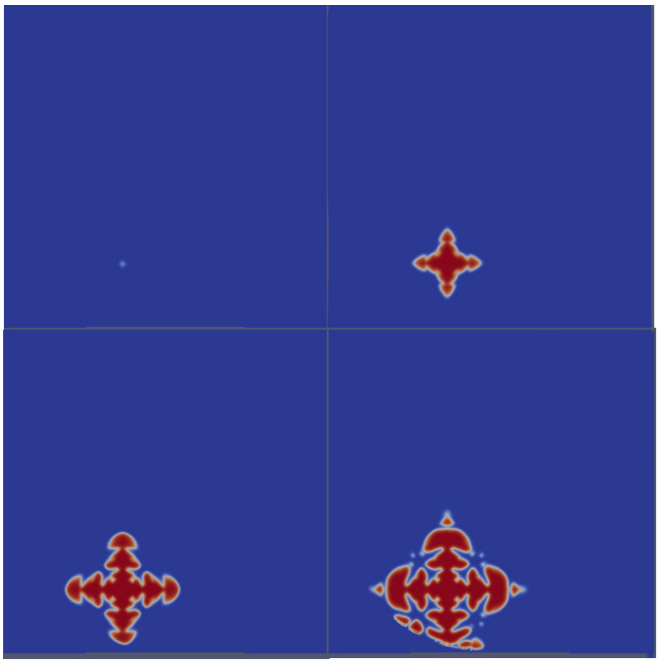

Fig. 3. Cross sections of 4 different stages of growth of a cross section of a crystal, with latent heat taken into account via a global heat balance. Top left is the crystal at 2000 microseconds into the simulation, top right is at 2500 microseconds, bottom left is at 3000 microseconds, and bottom right is at 3500 microseconds. In this image, red represents the solid phase of ϕ and blue the liquid and air phase. A slice showing the boundary of the droplet against the airfield is found in the Appendix.

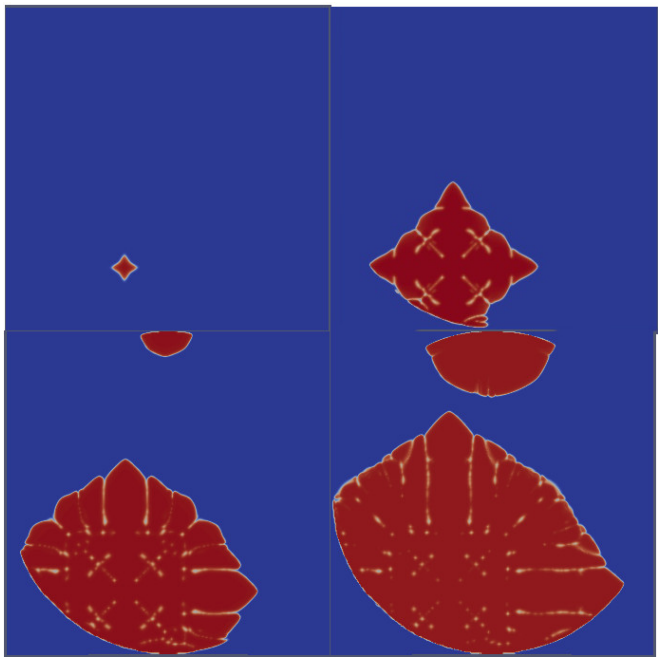

Fig. 4. 4 different stages of growth of a cross section of a crystal, with latent heat release neglected.Top left is the crystal at 2000 microseconds into the simulation, top right is at 2500 microseconds, bottom left is at 3000 microseconds, and bottom right is at 3500 microseconds. In this image, red represents the solid phase of ϕ and blue the liquid and air phase.

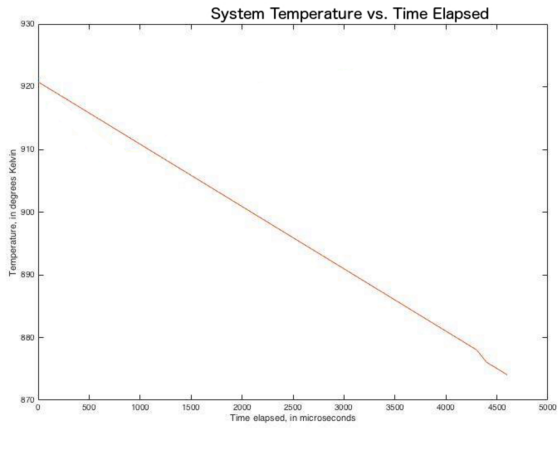

Fig. 5. The system temperature throughout the duration of the simulation without accounting for latent heat.

The results, as shown in Figures 6, 7 and 8, reveal even greater morphological and solidification rate differences than seen in Case 1. In the presence of global heat balance with no capillary anisotropy the dendrites tips are rounded, and growth away from the primary axes is relatively strong. By later time steps as shown in the bottom right of Figure 6, the morphology is complex but not systematically organized as it has some long thin branches (off the primary axes), when others are thick and round (along primary axes). When both global heat balance and capillary anisotropy were disabled, the growth rate was so high that after 4000 microseconds nearly the entire droplet was solidified (Figure 7). In Figure 8, smaller time steps demonstrate a very simple morphology with all slices, as the interface grows continuously without strong preferential growth direction. Although forming a diamond shape with tips along primary axes, all solidification fronts move so quickly that no intricate dendrites have time to form.

Comparing the results from both cases, there is clear morphological dependence on both the capillary anisotropy and the global heat balance. Without heat balance, both case 1 (Figure 4) and case 2 (Figures 7 and 8) show much higher rates of solidification, and very large solid structures without the expected dendritic morphology. The simulations with (Figure 3) and without (Figure 6) capillary anisotropy the growth is approximately the same when considering equal time steps (Figure 3, bottom right corner, and Figure 5, top right corner), however their morphology is very different. Without capillary anisotropy, the molecules do not take preference for crystallographic planes, suggesting they can align in unique ways. Figure 6 shows very unique crystallization, supporting this theoretical hypothesis. With the presence of latent heat fluctuating the temperature along the boundary, in Case 1, the molecules must re-melt and wait until there is a cold enough temperature along the preferential axes governed by the capillary anisotropy, where as in Case 2, they can solidify the presence of latent heat only redirects the growth into unusual places.

2. Conclusion

From these simulations we can conclude that the phase field model implemented by our code produces accurate and useful insight to the growth rate and morphologies of rapidly solidified Al-Cu alloy droplets. When the global heat balance is included, the growth of the crystals is slowed due to increased temperature at the interface. This falls in line with the theory established, as the slowed cooling rate leads to more dominant influence from the capillary anisotropy,

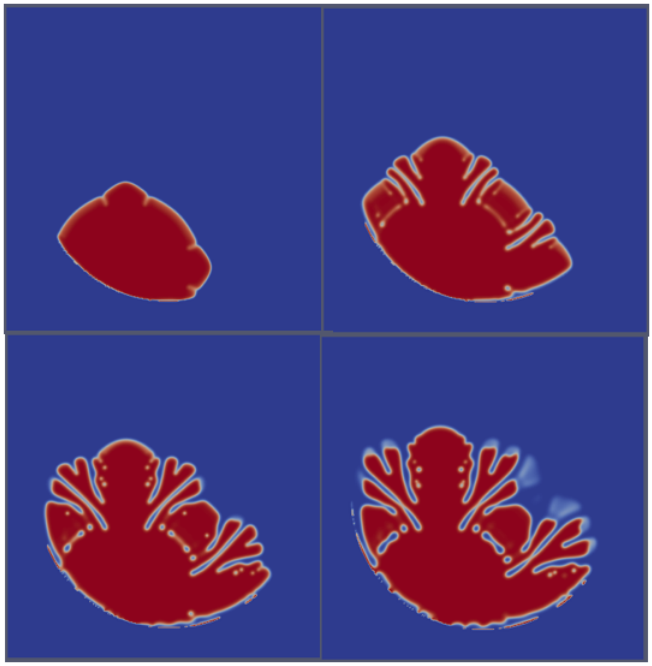

Fig. 6. Cross section of solidifying droplet after 2000, 3000, 4000, and 5000 microseconds (top left to bottom right). Simulating latent heat release without capillary anisotropy. In this image, red represents the solid phase of ϕ and blue the liquid and air phase.

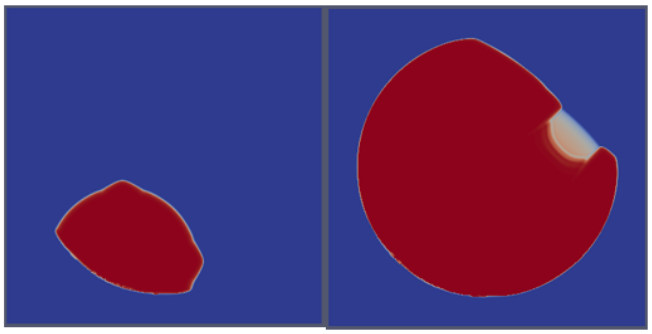

Fig. 7. Cross section of solidifying droplet after 2000 and 4000 microseconds (left to right) without latent heat release or capillary anisotropy. In this image, red represents the solid phase of ϕ and blue the liquid and air phase.

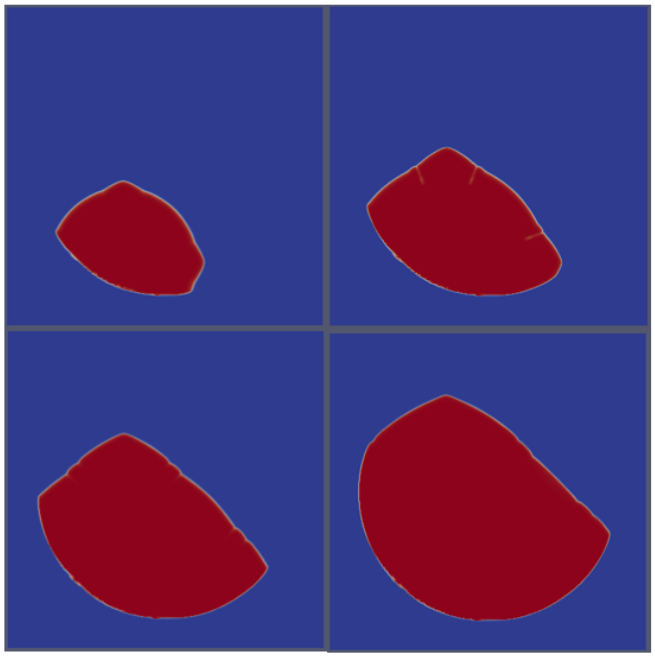

Fig. 8. 4 different stages of growth of a cross section of a crystal, with latent heat release neglected.

resulting in well defined dendritic branches. The lack of a heat balance leads to a faster growth from the nucleus in the radial direction, with a more limited influence from the capillary anisotropy. Crystal growth without heat balance as well as capillary anisotropy is, as expected, uncoupled with direction but is rapid in its growth, resulting in a blob-like shape. Thus it is evident that the inclusion of a global heat balance to account for latent heat release is necessary in order to accurately simulate crystal growth, but also in order create certain dendrite morphologies within the crystal. Further steps include simulations accounting for the influence of the kinetic anisotropy, as well as simulations in which the heat balance is paired with a rapid cooling rate. These simulations would lead to a more complete model that accurately represents the recrystallization phenomenon. Additionally, an accurate plot of the system temperature versus the elapsed time in simulations with global heat balance would allow a better assessment of how thermal fluctuations in the system affect morphology.

3. Materials and Methods

The phase field model was implemented using C++, with simulations being run on McGill University's Guillimin supercomputer. Slices and contours of the resulting simulation files were generated using a Python script, generated files were then analyzed using Paraview.

The alloy in question, Al 4.5 weight % Cu was used as there was extensive research and literature available on the alloy (3) (4). This is partly due to the alloys characteristics lending itself well to industrial processes, such as its lightness, durability, and price.

The parameters used throughout the simulations are defined below in Table 1, and were acquired in a variety of ways. Most were found in literature as many characteristics of the alloy had to have been found experimentally. Other parameters were computed. Graphs were created in MATLAB, and image editing in GIMP and PAGES.

Table 1. Parameters utilized in simulations.

Nominal composition of the alloy, C_o	$4.5 w.t.\%$	
Liquidus slope, m	$-2.6 K/w.t.$ %	(1)
Partition coefficient, k	0.14	(1)
Pure melting temperature of Aluminum, T_m	$933.47 K$	(1)
Gibbs-Thomson Coefficient, Γ	$2.4 * 10^{-7} Km$	(1)
Liquid diffusion coefficient, D_L	$3.0 * 10^{-9} m^2 s^{-1}$	(1)
Timescale, λ	8	
Capillary length, d_o	$2.385 * 10^{-8} m$	Eq [5]
Interface width, W	$2.1588 * 10^{-7} m$	Eq [6]
Coupling factor, a_1	$\frac{5\sqrt{2}}{8}$	(1)

$$d_o = \frac{\Gamma}{mC_o(1-k)} = 2.385 * 10^{-8} m \quad [5]$$

$$W = \frac{\lambda d_o}{a_1} \quad [6]$$

4. Acknowledgments

We acknowledge Dr. Nikolas Provatas for theory guidance, advice, patience, and computational resources.
We acknowledge Dr. Sabrina Leslie for paper formulation guidance.
We acknowledge Tatu Pinomaa (Technical Research Centre of Finland -VTT) for help with running the simulation code, as well as the code's maintenance.
We acknowledge Raj Shampur for simulation advice and code debugging, as well as general guidance.
We acknowledge Michael Greenwood CanmetMATERIALS (NRCAN) for access to the repository. Finally, we acknowledge Compute Canada as well as the McGill HPC Centre for their compuational resources.

5. References

1. Wang, Lei, Nan Wang, and Nikolas Provatas. *"Liquid Channel Segregation and Morphology and Their Relation with Hot Cracking Susceptibility during Columnar Growth in Binary Alloys."* Acta Materiala (2017): n. pag. Web.
2. Karma, Alain. *"Phase-Field Formulation for Quantitative Modeling of Alloy Solidification."* Physical Review Letters 87.11 (2001): n. pag. Web.
3. Bedel, M., G. Reinhart, Ch-A Gandin, A-A Bogno, H. Nguyen-Thi, and H. Henein. *"Evolution of the Dendritic Morphology with the Solidification Velocity in Rapidly Solidified Al-4.5wt.%Cu Droplets."* IOP Conference Series: Materials Science and Engineering 84 (2015): 012016. Web.
4. Bedel, M., G. Reinhart, A.-A. Bogno, Ch.-A. Gandin, S. Jacomet, E. Boller, H. Nguyen-Thi, and H. Henein. *"Characterization of Dendrite Morphologies in Rapidly Solidified Al-4.5wt.%Cu Droplets."* Acta Materialia 89 (2015): 234-46. Web.
5. Nele Moelans, Bart Blanpain, Patrick Wollants *"An introduction to phase-field modeling of microstructure evolution"* Calphad: (2008): Web.
6. Nikolas Provatas, Ken Elder *"Phase Field Methods in Material Science and Engineering."* (2001): Web.
7. Kenneth G. Libbrecht, "*SnowCrystals.com" Caltech: (1999): Web.*
8. "Dendridic Growth" University of Cambridge: (2004): Web.

6. Appendix

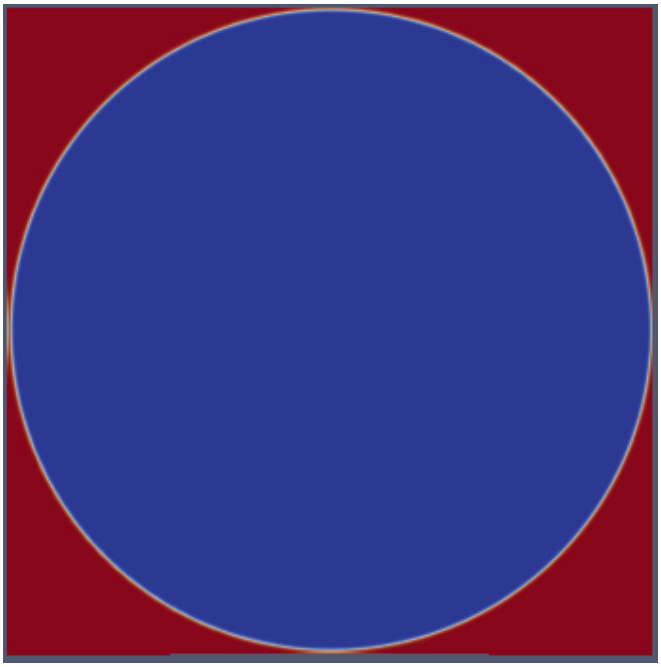

Fig. 9. Simulation boundary, blue represents the space in which the crystal is allowed to grow, while red represents the air field that surrounds the droplet.